ScieRxiv
NOT PEER-REVIEWED
Original Article

Long-term spatiotemporal variability of fine particulate matter ($PM_{2.5}$) across Idaho, USA, using statistical and geospatial tools

Mavia Anjum[1,*]

[1]Department of Physics, University of Idaho, Moscow, ID 83844, USA.

***Correspondence to:** Dr. Mavia Anjum, Department of Physics, University of Idaho, Moscow, ID 83844, USA. E-mail: manjum@uidaho.edu/mav.mavia14@gmail.com

Received: 12 October 2026 | Approved: 29 October 2026 | Online: 29 October 2026

Abstract

Fine particulate matter ($PM_{2.5}$) is a leading environmental risk factor for human health, driven in the interior Pacific Northwest by summertime wildfire smoke and wintertime residential wood combustion trapped by valley inversions. This study characterized the seasonal, spatial and temporal structure of $PM_{2.5}$ across Idaho, USA, over 2005 to 2024, and inferred its dominant source regimes using statistical and geospatial tools. The complete daily $PM_{2.5}$ record of the US Environmental Protection Agency Air Quality System was aggregated to 4,260 site-months for 32 sites, and Mann-Kendall and Theil-Sen trend analysis, Pearson correlation, principal component analysis (PCA) and inverse distance weighting (IDW) interpolation were applied. The regional mean was 7.53 µg m^{-3}, with a site range of 3.16 to 12.08 µg m^{-3}. The climatology was bimodal, with an August to September wildfire maximum and a November to February wood-smoke and inversion maximum separated by a clean spring background, and July to September carried 36.6 % of the annual mass. The cold-season and background series declined significantly, whereas the fire-season series rose at 2.54 µg m^{-3} per decade, which held the annual mean flat. PCA separated the network into two source regimes explaining 57.5 % of the between-site variance, and a temporal mode was dominated by

© The Author(s) 2026. Open Access This article is licensed under a Creative Commons Attribution 4.0 International License (https://creativecommons.org/licenses/by/4.0/), which permits unrestricted use, sharing, adaptation, distribution and reproduction in any medium or format, for any purpose, even commercially, as long as you give appropriate credit to the original author(s) and the source, provide a link to the Creative Commons license, and indicate if changes were made.

July to September episodes, identifying wildfire smoke as the dominant driver. It was found that 32.7 % of site-years exceeded the 2024 annual standard of 9.0 μg m^{-3}, and the two regimes are diverging under a warming climate, so that season and source specific management is required.

Keywords: PM2.5, wildfire smoke, wood combustion, principal component analysis, inverse distance weighting

1INTRODUCTION

Fine particulate matter with an aerodynamic diameter below 2.5 μm ($PM_{2.5}$) is among the most consequential environmental risk factors for human health worldwide[1,2]. A large body of epidemiological evidence links chronic $PM_{2.5}$ exposure to increased all-cause, cardiovascular and respiratory mortality. Each 10 μg m^{-3} increment in annual $PM_{2.5}$ was associated with a 7.3 % rise in all-cause mortality in a cohort of more than 60 million people[3], and the American Heart Association has formally recognized $PM_{2.5}$ as a modifiable cause of cardiovascular disease[4,5]. Beyond the particle mass itself, $PM_{2.5}$ acts as a carrier of adsorbed toxic heavy metals, including Pb, Cd, As, Cr and Ni, whose inhalation contributes additional carcinogenic and non-carcinogenic health burdens[6-8]. In recognition of this evidence, the World Health Organization set an annual $PM_{2.5}$ guideline of 5 μg m^{-3}[9], and in 2024 the United States Environmental Protection Agency (EPA) lowered the primary annual $PM_{2.5}$ National Ambient Air Quality Standard (NAAQS) from 12.0 to 9.0 μg m^{-3}, retaining the 24-h standard at 35 μg m^{-3}[10].

The western United States has experienced a marked intensification of wildfire, driven by anthropogenic warming and increasing fuel aridity[11,12], and a large share of recent ignitions is human-caused[13]. This intensification has produced a distinctive air-quality signature. Whereas $PM_{2.5}$ has declined across most of the country, a positive trend in the policy-relevant upper quantiles of $PM_{2.5}$ has been identified across the Northwest and tied to wildfire carbon[14]. Wildfire smoke now accounts for a growing fraction of total $PM_{2.5}$ and has offset regulatory gains in fire-prone regions[15-17]. Wildfire-derived $PM_{2.5}$ also appears more toxic per unit mass than $PM_{2.5}$ from other sources[18,19], and is associated with excess respiratory and cardiovascular morbidity and mortality[20-22].

A second and distinct source regime operates in the same region during winter. In the cold and topographically confined valleys of the northern Rocky Mountains, emissions from residential wood combustion accumulate beneath persistent cold-air pools and temperature inversions[23,24]. Under such conditions $PM_{2.5}$ can build up at roughly 6 to 10 µg m^{-3} per day over multi-day episodes[25-27]. Idaho contains numerous analogous airsheds, including the Silver Valley, the central mountain valleys and the towns of the Snake River Plain, yet the interplay of these two regimes across the full monitoring network of the State has not been synthesized over a multi-decadal period.

Multivariate and geospatial tools are well established for resolving particulate sources and mapping their distribution. Principal component analysis (PCA)[28,29], positive matrix factorization[30], Pearson correlation and inverse distance weighting (IDW) interpolation[31] have been applied to particulate and elemental datasets to identify covarying source components and their spatial patterns, including in previous work on the industrial area of Islamabad[6,32]. When speciated composition is unavailable, the space and time structure of the $PM_{2.5}$ mass field itself retains a strong imprint of the underlying source processes. A state-scale synthesis of Idaho $PM_{2.5}$ that jointly resolves the seasonal source regimes, quantifies their divergent long-term trends and maps their spatial distribution has not previously been reported. The objective of this study is to characterize the seasonal, spatial and temporal structure of $PM_{2.5}$ across Idaho over 2005 to 2024 and, using Pearson correlation, PCA and IDW interpolation, to infer the dominant source regimes and to quantify the behaviour of $PM_{2.5}$ during the wildfire season.

EXPERIMENTAL

Description of the study area

Idaho spans approximately 42 to 49° N and 111 to 117° W across the interior Pacific Northwest, covering about 216,000 km^2. Its terrain is deeply dissected, with numerous enclosed mountain valleys in the north and centre and the broad and semi-arid Snake River Plain in the south. This physiography controls both the wintertime accumulation of local emissions through cold-air pooling and inversions, and the intrusion of transported wildfire smoke. Summers are warm and fire-prone, whereas winters are cold with frequent stable layers. The regulatory $PM_{2.5}$ network samples a wide range of environments, from densely populated valley towns to remote high-elevation and rural

background sites. Site latitudes analyzed here ranged from 42.08° N at Preston to 48.29° N at Sandpoint.

Data acquisition and processing

The complete Idaho $PM_{2.5}$ record for 2005 to 2024 was retrieved from the EPA Air Quality System (AQS) through its programmatic interface, comprising daily summary data for the Local Conditions parameters 88101 (Federal Reference and Equivalent Method, gravimetric and continuous FEM) and 88502 (continuous non-FEM mass used for the Air Quality Index). The full inventory contained 43 sites, of which 32 returned usable monthly aggregates. Site coordinates were taken from the AQS station metadata. Records were resolved to a single value per site, day and monitor by prioritizing 24-h sample durations. Where exceptional-event flags were present, the measured concentration was retained so that wildfire-smoke impacts on exposure were preserved. Daily values were aggregated to calendar-month means, and a single series per physical site was formed by preferring parameter 88101 where available and substituting 88502 otherwise, which maximized spatial and temporal coverage. This procedure yielded 4,260 site-months across 32 sites. Five sites provided the full 240 months, 16 provided at least 120 months and 24 provided at least 60 months. Computations were performed in Python using the NumPy, pandas and SciPy libraries.

Descriptive climatology

The regional monthly climatology was computed by pooling all available site-months for each calendar month. The 95 % confidence interval (CI) of each monthly mean was obtained from the Student t distribution as in Eq. (1), where $\bar{x}$ is the sample mean, s the standard deviation, n the number of site-months and t the critical value at the 0.975 quantile with n minus 1 degrees of freedom.

$$95\%\ CI = \bar{x} \pm t_{0.975,\,n-1}\ \frac{s}{\sqrt{n}} \tag{1}$$

Mann-kendall trend test and Theil-Sen slope

Monotonic trends in the regional annual and seasonal series were tested with the non-parametric Mann-Kendall statistic S[33] given in Eq. (2), where x_j and x_k are sequential values and n is the series length. The standardized statistic Z in Eq. (3) refers to the standard normal distribution, and τ equal to S divided by n(n minus 1)/2 measures the

strength of the trend. Rates of change were estimated with the non-parametric Theil-Sen slope[34] in Eq. (4), the median of the pairwise slopes between all data pairs, which is robust to outliers and to the episodic nature of smoke.

$$S=\sum_{k=1}^{n-1}\sum_{j=k+1}^{n}\operatorname{sgn}\left(x_j-x_k\right) \tag{2}$$

$$Z=\frac{S-1}{\sqrt{Var(S)}}\ (S>0),\quad Z=\frac{S+1}{\sqrt{Var(S)}}\ (S<0) \tag{3}$$

$$\beta=\text{median}\left[\frac{x_j-x_i}{j-i}\right],\quad i<j \tag{4}$$

Pearson correlation and principal component analysis

Inter-site association was quantified with the Pearson correlation coefficient r in Eq. (5) on pairwise-complete monthly series with a minimum of 24 overlapping months, computed on the raw series and on deseasonalized anomalies obtained by removing each calendar-month climatology. Here a_i and c_i are paired observations and $\bar{a}$ and $\bar{c}$ their means.

$$r=\frac{\sum_i\ (a_i-\bar{a})\,(c_i-\bar{c})}{\sqrt{\sum_i\ (a_i-\bar{a})^2\ \sum_i\ (c_i-\bar{c})^2}} \tag{5}$$

Principal component analysis reduces a set of inter-correlated variables into a smaller number of orthogonal components that retain most of the variance[28]. Two analyses were performed. The first, denoted PCA-A, was applied to the matrix of site seasonal-shape profiles of 24 sites by 12 calendar months, with each profile standardized within site, to classify sites by seasonal regime. The second, denoted PCA-B, was a temporal empirical orthogonal function applied to the standardized deseasonalized anomaly field of the 16 long-record sites, to resolve dominant modes of regional temporal covariability. This mass-only decomposition is complementary to, but does not substitute for, receptor models that require speciated inputs[29,30].

Inverse distance weighting interpolation

The spatial distribution of the monthly and annual site means was mapped with inverse distance weighting (IDW) interpolation in ESRI ArcGIS[31,32]. The estimate F(z) at an unsampled point is a distance-weighted linear combination of the known values z_i in Eq. (6), where the weight w_i decays with distance d_i raised to a power p.

$$F(z)=\frac{\sum_i w_i z_i}{\sum_i w_i}, \quad w_i=d_i^{-p} \tag{6}$$

Four seasonal windows were examined, namely the full year, the fire season from July to September, the cold season from November to February, and the spring background from April to June. The fire-season share was defined as the July to September sum of monthly means divided by the annual sum, expressed as a percentage. Because monthly air-quality series can be serially correlated, the reported *p*-values are treated as indicative, and inference is anchored on the contrast between seasons.

RESULTS AND DISCUSSION

Regional climatology and seasonality

The regional monthly climatology was found to be distinctly bimodal [Figure 1]. The primary maximum occurred in August and September, at 13.28 and 11.68 µg m^{-3} respectively, with a 95 % CI for August of 12.36 to 14.20 µg m^{-3}. This maximum coincided with the wildfire season. A secondary maximum spanned the cold months and peaked in January at 8.78 µg m^{-3}, with comparable values in November and December of 8.51 and 8.45 µg m^{-3} respectively. The two maxima were separated by a clean April to June background of 4.11 to 4.16 µg m^{-3}. It was found that July to September alone contributed 36.6 % of the summed monthly-mean mass, with August contributing 14.7 %. The amplitude of the cycle was pronounced, as the August maximum exceeded the June minimum by a factor of 3.2, and the summer and winter maxima were of comparable magnitude, so that no single season dominated the annual budget. The dispersion also differed sharply between seasons. The standard deviation was 8.87 µg m^{-3} in August and 10.71 µg m^{-3} in September, against only 1.63 to 1.78 µg m^{-3} in April to June, which confirms that the summer maximum is driven by a small number of intense and episodic months rather than by a uniform seasonal elevation. This two-peaked structure is the empirical foundation for the two-regime interpretation developed below, and it is consistent with the coexistence of a transported-smoke source and a local combustion and inversion source documented for the wider region[24,35]. Monthly statistics are reported in Table 1.

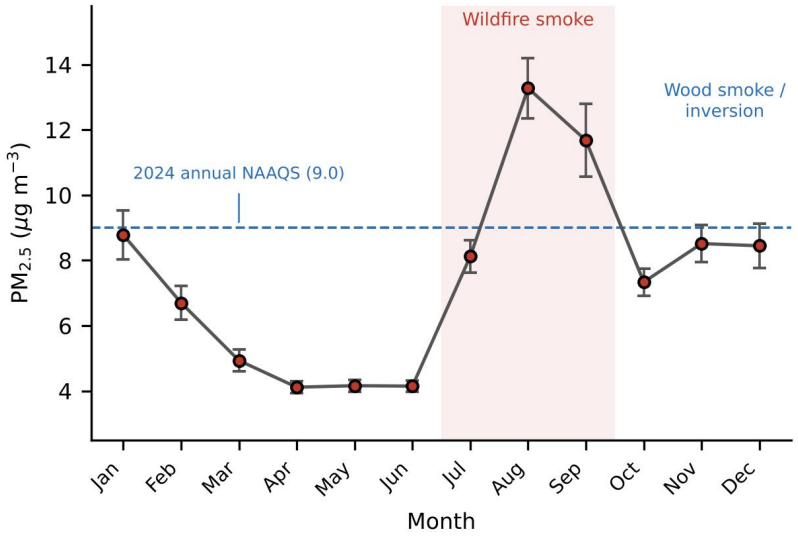


Figure 1. Regional monthly climatology of PM2.5 across Idaho over 2005 to 2024, pooled over all available site-months. Markers are monthly means and error bars are 95 % confidence intervals. The shaded band marks the July to September fire season and the dashed line the 2024 annual NAAQS of 9.0 µg m^{-3}.

Table 1. Regional monthly climatology of PM2.5 (µg m^{-3}): mean, standard deviation, 95 % confidence interval and number of pooled site-months.

Month	Mean	SD	95 % CI	*n*
January	8.78	7.08	8.03 to 9.53	345
February	6.70	4.93	6.18 to 7.22	346
March	4.93	3.18	4.59 to 5.27	345
April	4.11	1.78	3.93 to 4.30	356
May	4.16	1.72	3.98 to 4.34	359
June	4.15	1.63	3.98 to 4.32	358
July	8.12	4.77	7.62 to 8.62	354
August	13.28	8.87	12.36 to 14.20	358
September	11.68	10.71	10.56 to 12.79	358
October	7.34	4.03	6.92 to 7.75	358
November	8.51	5.43	7.95 to 9.08	363
December	8.45	6.55	7.77 to 9.13	360

Spatial distribution and site-level burden

Site long-term means spanned nearly a factor of four, from 3.16 µg m^{-3} at Craters of the Moon National Monument and 3.63 µg m^{-3} at Sawtooth National Forest to 12.08 µg m^{-3} at Pinehurst in the Silver Valley, 11.96 µg m^{-3} at Salmon and 10.23 µg m^{-3} at St. Maries [Table 2]. Against the regulatory thresholds, 32.7 % of the 196 site-years with valid annual means exceeded the 2024 annual standard of 9.0 µg m^{-3}, 6.1 % exceeded the former 12.0 µg m^{-3} standard, and 27.0 % showed a 98th-percentile 24-h value above 35 µg m^{-3}. Individual fire-season months reached extreme levels. The Salmon monthly mean attained 103.9 µg m^{-3} in September 2012, with a peak daily value of 214 µg m^{-3}, and in the September 2020 West-Coast smoke episode daily maxima reached 276 µg m^{-3} at Pinehurst and 313 µg m^{-3} at Lewiston, which are values in the hazardous range[19].

Table 2. Inventory of the 24 well-characterized monitoring sites with at least 60 months of data, ordered north to south, with coordinates, record span, number of site-months, long-term mean PM2.5 (µg m^{-3}) and the source regime assigned from the PCA-A seasonal-shape score.

Site	County	Lat	Lon	Span	Months	Mean	Regime
Sandpoint	Bonner	48.29	-116.56	2015-2023	98	8.9	Fire/background
Pinehurst	Shoshone	47.54	-116.24	2005-2024	240	12.1	Wood/inversion
St. Maries	Benewah	47.32	-116.57	2005-2024	240	10.2	Wood/inversion
Moscow	Latah	46.72	-116.96	2005-2024	213	5.0	Fire/background
Lewiston	Nez Perce	46.41	-116.99	2005-2024	216	7.2	Fire/background

Site	County	Lat	Lon	Span	Months	Mean	Regime
Lapwai	Nez Perce	46.40	-116.81	2015-2024	110	5.6	Fire/background
Kamiah	Idaho	46.21	-116.03	2005-2024	146	9.0	Wood/inversion
Grangeville	Idaho	45.93	-116.12	2005-2024	213	6.0	Fire/background
Salmon	Lemhi	45.18	-113.89	2005-2024	240	12.0	Wood/inversion
McCall	Valley	44.89	-116.11	2005-2024	153	8.3	Wood/inversion
Sawtooth NF	Custer	44.17	-114.93	2005-2024	240	3.6	Fire/background
Garden Valley	Boise	44.10	-115.97	2005-2024	134	8.5	Fire/background
Idaho City	Boise	43.82	-115.84	2005-2024	148	9.1	Wood/inversion
Ketchum	Blaine	43.68	-114.37	2015-2024	103	5.1	Fire/background
Ada Co. Fairgrounds	Ada	43.65	-116.21	2019-2024	65	8.0	Wood/inversion

Site	County	Lat	Lon	Span	Months	Mean	Regime
Meridian	Ada	43.60	-116.35	2006-2024	222	8.4	Wood/inversion
Nampa Fire Station	Canyon	43.58	-116.56	2008-2023	178	9.6	Wood/inversion
Idaho Falls	Bonneville	43.46	-112.05	2015-2024	113	6.6	Fire/background
Craters of the Moon	Butte	43.46	-113.56	2005-2024	240	3.2	Fire/background
Ballard Road	Bannock	42.98	-112.46	2008-2020	139	6.4	Fire/background
Pocatello	Bannock	42.88	-112.46	2005-2024	175	5.8	Wood/inversion
Twin Falls	Twin Falls	42.57	-114.49	2015-2024	116	6.7	Fire/background
Smiths (Twin Falls)	Twin Falls	42.56	-114.45	2005-2013	107	6.7	Wood/inversion
Preston	Franklin	42.08	-111.86	2005-2024	117	6.5	Wood/inversion

Long-term and seasonal trends

The state-wide annual mean showed no significant trend over 2005 to 2024, with a Mann-Kendall τ of -0.084 and p of 0.63 and a Theil-Sen slope of -0.017 μg m^{-3} yr^{-1}, but

this stability masked strongly divergent seasonal behaviour [Figure 2, Table 3]. The cold-season series declined significantly, with τ of -0.40 and p of 0.015 and a rate of -0.92 μg m^{-3} per decade, as did the spring background, with τ of -0.44 and *p* of 0.007 and a rate of -0.69 μg m^{-3} per decade. In direct contrast, the fire-season series increased at 2.54 μg m^{-3} per decade, with τ of 0.23 and *p* of 0.16, the trend not attaining significance owing to the large interannual variability of smoke. The declining cold-season and background burdens were therefore offset by a rising fire-season contribution, which held the annual mean flat. This divergence is a state-level expression of the national pattern in which $PM_{2.5}$ improves except in wildfire-prone regions[14,16,17]. The practical implication is that an annual-mean metric conceals two opposing and policy-relevant trajectories, so that the apparent stability of the Idaho record should not be read as an absence of change.

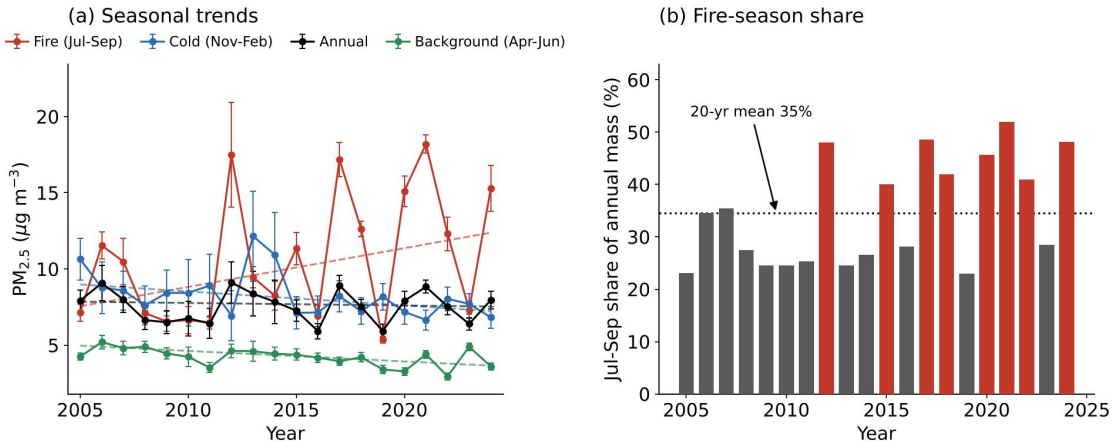


Figure 2. (a) Regional annual and seasonal PM2.5 series over 2005 to 2024 with standard-error bars and Theil-Sen trend lines, for the fire season (July to September), the full year, the cold season (November to February) and the spring background (April to June); (b) July to September share of the summed annual monthly-mean mass by year, with bars of at least 40 % highlighted and the dotted line showing the 20-year mean.

Table 3. Seasonal trend statistics for regional PM2.5 over 2005 to 2024: long-term mean, Mann-Kendall τ and *p*, Theil-Sen slope and change per decade.

Window	Mean	τ	*p*	Slope (yr-1)	Per decade	Significant
Annual (Jan-Dec)	7.54	-0.084	0.626	-0.017	-0.17	no

Window	Mean	τ	*p*	Slope (yr-1)	Per decade	Significant
Fire season (Jul-Sep)	10.64	0.232	0.163	+0.254	+2.54	no
Cold season (Nov-Feb)	8.29	-0.400	0.015	-0.092	-0.92	yes
Background (Apr-Jun)	4.21	-0.442	0.007	-0.069	-0.69	yes

Fine particulate matter during the fire season

The July to September window was the principal determinant of the $PM_{2.5}$ exposure of Idaho in most recent years. The fire-season share of the annual mass rose from 23 to 25 % in low-smoke years such as 2005, 2011 and 2019 to between 48 and 52 % in severe fire years, reaching 51.9 % in 2021, 48.6 % in 2017, 48.1 % in 2024, 48.0 % in 2012 and 45.7 % in 2020 [Figure 2b]. The fire-season mean of 10.64 μg m^{-3} exceeded both the cold-season mean of 8.29 μg m^{-3} and the background mean of 4.21 μg m^{-3}. The magnitude and direction of this change are consistent with the growing wildfire contribution to United States $PM_{2.5}$[15,16,36] and with the emergence of a new seasonal pollution pattern over North America[37]. The fire-season series was also far more variable from year to year than the cold-season or background series, which reflects the episodic and meteorology-gated nature of smoke transport. The July to September share ranged from 23.0 % in the low-smoke year 2019 to 51.9 % in 2021, a spread of more than a factor of two that is driven by the interannual severity of regional fire activity rather than by local emissions. Because wildfire $PM_{2.5}$ is disproportionately harmful per unit mass[18], the rising fire-season share implies a health burden that grows faster than the mass trend alone would suggest.

Inter-site correlation structure

The 16 long-record sites were strongly and positively correlated. Raw monthly correlations averaged r of 0.58, dominated by the shared seasonal cycle. After deseasonalization, the anomaly correlations remained high, with a mean r of 0.51 and a range of 0.07 to 0.93, which demonstrates that anomalous months at one site coincide with anomalous months elsewhere. This synchrony is the signature of a regional forcing

rather than of isolated local sources. The correlation was also spatially organized. The mean anomaly correlation within northern Idaho of 0.67 exceeded that within southern Idaho of 0.51 and the north to south cross-correlation of 0.46, which indicates a distance-decaying coherence superimposed on the state-wide signal. In Figure 3 each cell is rendered as a pie whose filled fraction is proportional to the absolute value of r, so that the pervasive and distance-modulated coherence of the network is directly visible.

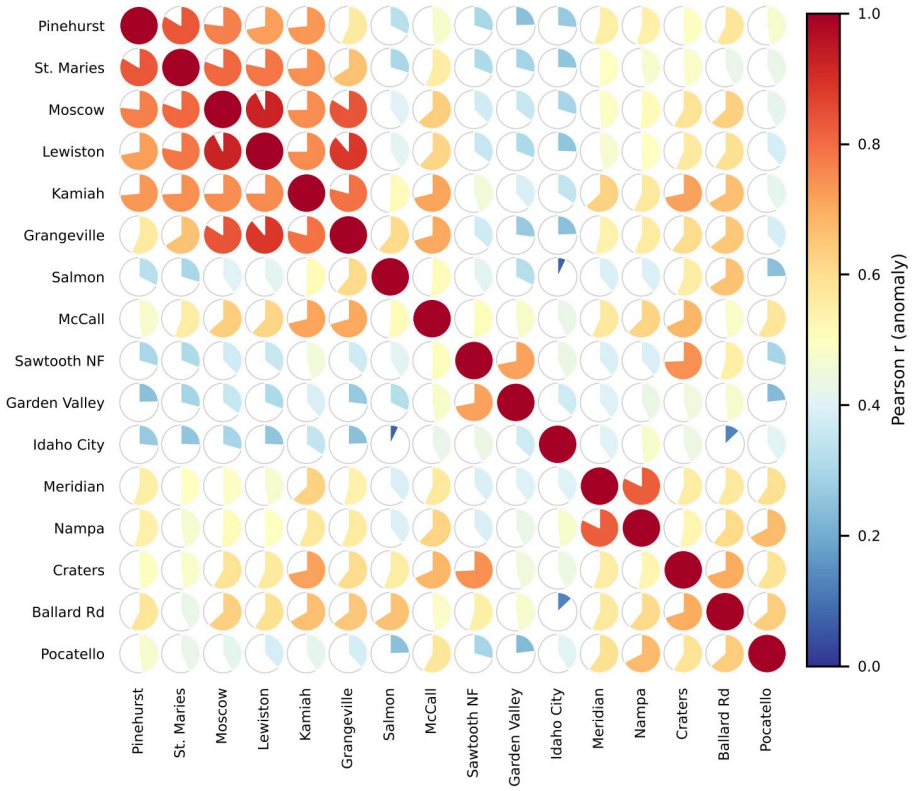


Figure 3. Pie-glyph correlation matrix of deseasonalized monthly PM2.5 anomalies among the 16 long-record sites, ordered north to south. Each pie is filled clockwise in proportion to the absolute value of r and coloured by the correlation value. The near-full and warm-coloured pies indicate synchronized month-to-month anomalies across the network, strongest among the northern sites.

Source regimes from principal component analysis

Principal component analysis of the site seasonal-shape profiles (PCA-A) resolved the network along a single dominant axis that explained 57.5 % of the between-site variance, with a second component that explained 22.4 % [Table 4]. The first component loaded

negatively on the winter months, at -0.44 for December, -0.43 for January and -0.32 for November, and positively on the summer months, at 0.42 for August, 0.27 for September and 0.26 for July. It therefore contrasts winter-peaking sites, which carry negative scores, with summer-peaking sites, which carry positive scores. The winter-peaking group comprised the high-concentration valley towns of Pinehurst at -3.18, St. Maries at -2.09, Idaho City at -1.99, Salmon at -1.73 and McCall at -1.07. The summer-peaking group comprised the low-concentration remote and high-elevation sites of Craters of the Moon at 2.14, Sawtooth National Forest at 2.05, Moscow at 1.65, Grangeville at 1.27 and Ketchum at 1.08. Because the first-component score was inversely related to the overall site level, the two regimes are also the dirty-winter and the clean-background ends of the network.

The temporal empirical orthogonal function (PCA-B) yielded a leading mode that explained 50.0 % of the regional anomaly variance and on which every site loaded with the same sign, which is a single and coherent state-wide mode. Its ten largest excursions all occurred in July to September, led by September 2020, September 2017, August 2015, July and August 2021, September 2012, September 2022, August 2017, July 2024 and August 2018 [Figure 4]. The concurrence of the leading regional mode with the wildfire calendar identifies wildfire smoke as the principal driver of month-to-month $PM_{2.5}$ variability across Idaho[17,35]. The two regimes are therefore wintertime residential wood combustion trapped by inversions[23-25] and summertime wildfire smoke[14,16]. A formal apportionment of their relative contributions would require speciated measurements and a receptor model[29,30].

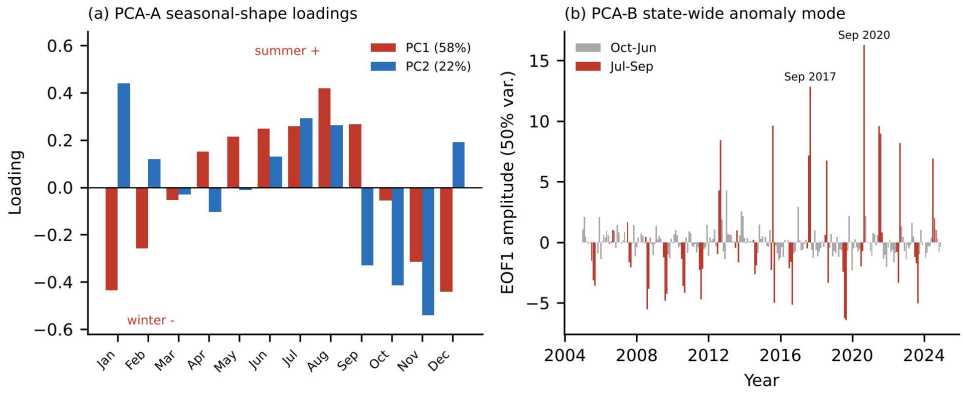


Figure 4. (a) PCA-A seasonal-shape loadings. The first component contrasts summer-positive with winter-negative months, and the second separates autumn from deep-

winter and midsummer peaking; (b) Temporal amplitude of the leading empirical orthogonal function of the deseasonalized anomaly field (PCA-B), with July to September months highlighted. Every one of the ten largest excursions falls in the fire season.

Table 4. PCA-A monthly loadings on the first two components. PCA-A explained variance for PC1 to PC4 was 57.5, 22.4, 6.3 and 5.1 %, and PCA-B explained variance for the first mode was 50.0 %.

Month	PC1 loading	PC2 loading
Jan	-0.43	+0.44
Feb	-0.26	+0.12
Mar	-0.05	-0.03
Apr	+0.15	-0.10
May	+0.22	-0.01
Jun	+0.25	+0.13
Jul	+0.26	+0.29
Aug	+0.42	+0.26
Sep	+0.27	-0.33
Oct	-0.06	-0.41
Nov	-0.32	-0.54
Dec	-0.44	+0.19

Spatial distribution of monthly and annual PM2.5

The IDW surfaces spatialize the two regimes [Figures 5 and 6]. Each monthly panel is stretched to its own range, so colours are compared through the printed High and Low values rather than across panels. In winter, in January to March and December, the surfaces show the steepest gradients and the highest local maxima over the enclosed northern valleys of the Silver Valley and St. Maries and over the east-central Salmon and Lemhi valley, with January spanning about 0.9 to 21.8 µg m^{-3} and December 1.0 to 18.9 µg m^{-3}, which is the spatial signature of wood combustion under inversions[24,25]. In spring, in April to June, the surfaces are lowest and most uniform, at 2.0 to 7.1, 2.4 to 8.0 and 2.6 to 9.2 µg m^{-3} respectively. In summer, in July to September, concentrations are elevated state-wide with high minima, as the cleanest interpolated area still reaches

8.4 µg m^{-3} in August, which is the broad pattern of transported wildfire smoke[14,17]. The annual surface in Figure 6 ranges from 3.16 to 12.07 µg m^{-3} and is dominated by the Silver Valley and the Salmon and Lemhi hotspots, and is cleanest over the Snake River Plain and the central wilderness. Interpolated values in the sparsely monitored central region are weakly constrained[31].

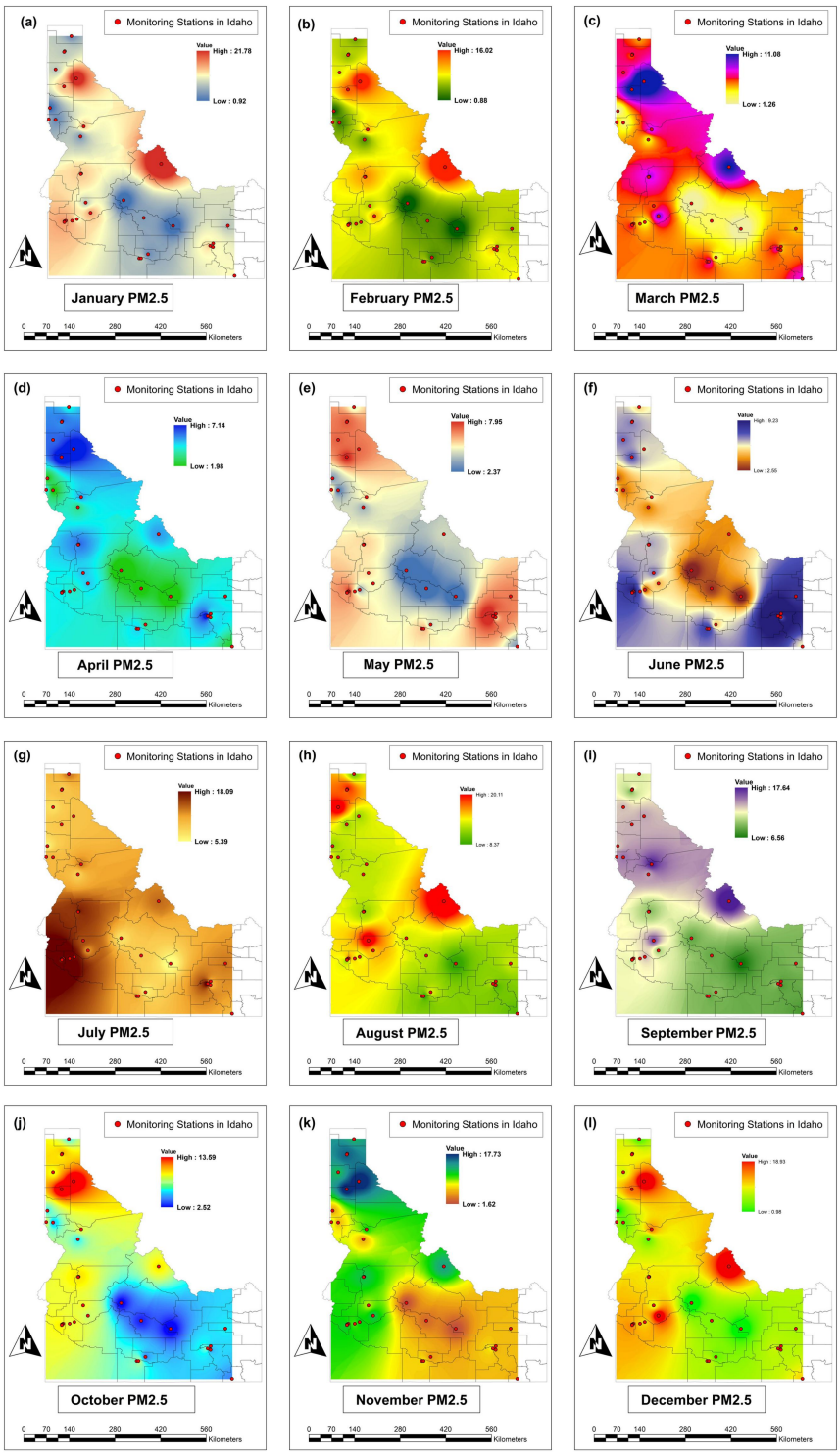


Figure 5. Interpolated (IDW) monthly PM2.5 surfaces for Idaho, from the 2005 to 2024 means, arranged by season with rows for winter, spring, summer and autumn. Red points are monitoring stations. Each panel is independently stretched to its own High and Low range, so the colours are not comparable across months.

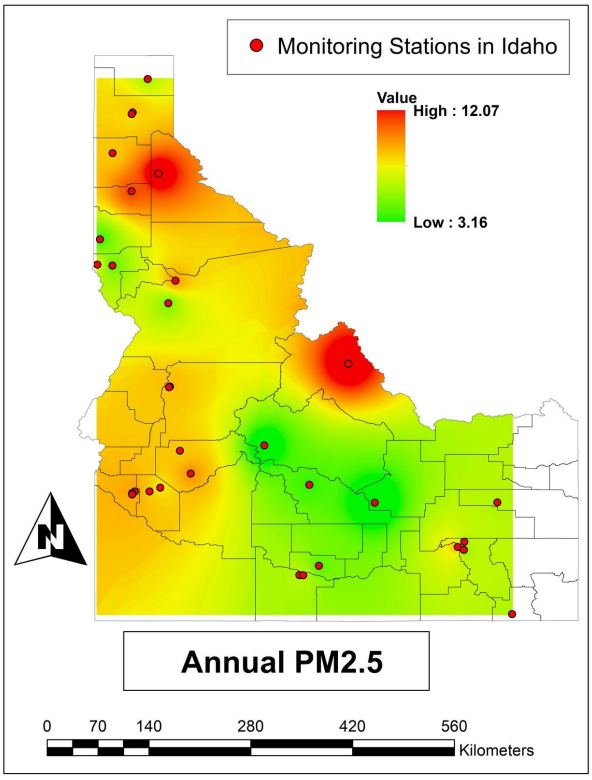


Figure 6. Interpolated (IDW) annual-mean PM2.5 surface for Idaho over 2005 to 2024, which ranges from 3.16 to 12.07 µg m-3 and is dominated by the northern Silver Valley and the east-central Salmon and Lemhi valley.

Comparison with air-quality standards and worldwide studies

The regional mean of 7.53 µg m^{-3} in Idaho lies between the WHO annual guideline of 5.0 µg m^{-3}[9] and the 2024 EPA annual standard of 9.0 µg m^{-3}[10]. A third of the site-years exceeded the latter, and the August peak of 13.3 µg m^{-3} exceeded even the former 12.0 µg m^{-3} standard. A comparison of the $PM_{2.5}$ burden measured in this study with values reported for cities and regions around the world is given in Table 5. The levels in Idaho are modest in a global context. The regional mean is about half of the mean of 15.1 µg m^{-3} reported for Islamabad[8] and far below the industrial area of the same city at 40.4 µg m^{-3}[6] and the value of 55.5 µg m^{-3} reported for Lahore[38]. The contrast is even sharper against the most heavily polluted megacities, where annual means reach 83

μg m^{-3} in Beijing[39] and 100 μg m^{-3} in Delhi[40]. The Idaho mean is also lower than the values reported for São Paulo at 28.1 μg m^{-3}[41], Kampala at 39 μg m^{-3}[42] and Milan at 41.9 μg m^{-3}[43], and is comparable to the recent decline in central Los Angeles from 15.4 to 10.5 μg m^{-3}[44]. What distinguishes Idaho is therefore not its annual mean but the episodic wildfire and inversion extremes, during which daily concentrations reach the hazardous range, comparable to the multi-day valley episodes documented elsewhere in the western United States[25,26]. This comparison reframes the Idaho record as one of a low-background and extremes-driven airshed rather than a chronically polluted one, which has direct consequences for how exposure should be managed.

Table 5. Comparison of the annual mean PM2.5 concentration (μg m^{-3}) measured in this study with values reported for cities and regions around the world.

Location	Period	PM2.5	Reference
Idaho, USA	2005-2024	7.5 (3.2-12.1)	This study
Los Angeles, USA	2014-2024	15.4 to 10.5	[44]
Islamabad, Pakistan	2008-2009	15.1	[8]
Sao Paulo, Brazil	2007-2008	28.1	[41]
Kampala, Uganda	2018-2021	39	[42]
Islamabad (industrial), Pakistan	2023	40.4	[6]
Milan, Italy	2003	41.9	[43]
Lahore, Pakistan	2019	55.5	[38]
Beijing, China	2013-2015	83	[39]
Delhi, India	2021-2022	100	[40]

Values are annual or study-period means as reported in the cited sources. For Los Angeles the range is the reported start-to-end decline over 2014 to 2024.

Health hazards

The exceedance statistics translate directly into a public-health concern. It was found that 32.7 % of the 196 site-years exceeded the 2024 annual standard of 9.0 μg m^{-3}, and every site exceeded the WHO annual guideline of 5.0 μg m^{-3}[9,10], so that essentially the entire monitored population of Idaho is chronically exposed above the level judged protective of health. On the concentration and response evidence, each 10 μg m^{-3} increment in annual $PM_{2.5}$ has been associated with a 7.3 % increase in all-cause mortality[3], and long-term exposure is an established cause of cardiovascular and

respiratory morbidity and mortality[1,2,4,5]. Applied in an illustrative way, the difference of about 9 µg m^{-3} between the cleanest site at Craters of the Moon, at 3.16 µg m^{-3}, and the dirtiest site at Pinehurst, at 12.08 µg m^{-3}, corresponds to a substantial difference in attributable chronic mortality risk between communities within the same State.

The fire-season burden is of particular concern because of its composition as well as its magnitude. Wildfire smoke is enriched in fine organic and black carbon and in polycyclic aromatic hydrocarbons, and per unit mass it is more damaging to respiratory health than $PM_{2.5}$ from other sources[18,19]. Short-term exposure to wildfire $PM_{2.5}$ has been linked to increased respiratory and cardiovascular hospitalizations and to excess mortality across hundreds of global locations[20,21,45], with children, older adults, pregnant women and people with pre-existing cardiopulmonary disease the most vulnerable subgroups[19,22]. During the September 2012 and September 2020 episodes documented here, daily maxima reached 214 to 313 µg m^{-3} at Salmon, Pinehurst and Lewiston, well within the hazardous Air Quality Index range, at which acute effects are expected even in otherwise healthy individuals.

The winter regime carries its own hazards. Residential wood smoke contains carbon monoxide, benzene and several carcinogenic compounds, and elevated wood-smoke $PM_{2.5}$ is causally associated with adverse respiratory outcomes, particularly in young children[23]. In addition, the $PM_{2.5}$ mass acts as a carrier of adsorbed toxic heavy metals, including Pb, Cd, As, Cr and Ni, whose inhalation adds both carcinogenic risk, from As, Cd, Cr(VI) and Ni, and non-carcinogenic risk, for example Pb neurotoxicity and Cd nephrotoxicity. Source-resolved measurements in an industrial setting found such metals concentrated in the fine fraction and traceable to combustion and industrial sources[6-8,32]. Because the fire-season share of the $PM_{2.5}$ of Idaho is rising while the annual mean is flat, the composition-weighted health burden is increasing faster than the mass trend alone would indicate, and an annual-mean metric understates the trajectory of the exposure most relevant to acute health effects.

Preventive and mitigation measures

The two regimes call for distinct and season-specific interventions. For the wintertime wood-smoke and inversion burden, source control is both effective and feasible. Residential wood-stove change-out and upgrade programmes, mandatory no-burn

advisories issued on forecast inversion days, a shift toward cleaner heating fuels, and home weatherization to reduce heating demand have all lowered wintertime $PM_{2.5}$ in comparable valley communities of the northern Rocky Mountains[23,24]. Because these episodes build gradually over several days as the cold-air pool strengthens[25,27], they are forecastable, and burn-ban messaging keyed to the valley heat deficit can pre-empt the worst accumulation. For the fire-season burden, which is largely exogenous and transported, exposure mitigation is the primary lever. Timely public alerts through the Air Quality Index, the designation and equipping of clean-air shelters with high-efficiency filtration, the distribution of portable air cleaners and well-fitted respirators, guidance to limit outdoor exertion during smoke events, and the specific protection of schools, outdoor workers and other sensitive settings are all effective[19,22]. At the landscape scale, fuel-reduction treatments, managed and prescribed burning under favourable dispersion conditions, and wildland and urban interface planning address the underlying driver of the summer regime[15,35]. It is recommended that the air-quality agencies of Idaho concentrate inversion and smoke forecast messaging together with clean-air-shelter networks in the high-burden airsheds identified here, namely the northern Silver Valley and the Salmon and Lemhi valley, where the two regimes are most intense.

Strengths, limitations and recommendations

The strengths of this study are its use of the complete two-decade AQS record for an entire state and the integration of statistical tools, namely Mann-Kendall, Theil-Sen, Pearson and PCA, with the geospatial IDW method, to jointly resolve the seasonality, the trends, the covariance structure and the spatial distribution of $PM_{2.5}$. Several limitations apply. First, the analysis used $PM_{2.5}$ mass without chemical speciation, so the source attribution is inferential rather than a formal receptor-model apportionment[29,30]. Second, the combination of parameters 88101 and 88502 maximizes coverage but mixes federal reference and equivalent measurements with continuous non-FEM measurements. Third, monthly aggregation removes the sub-monthly structure of individual episodes. Fourth, the network changed over the period, and the reported Mann-Kendall p-values are not corrected for serial correlation[33,34]. Finally, the IDW interpolation over the sparsely monitored central wilderness is weakly constrained[31]. It is recommended that future work incorporate speciated and continuous measurements to apportion the sources formally, extend the analysis to co-located

meteorology and smoke products, and evaluate the health burden of the two regimes separately.

CONCLUSIONS

The complete 2005 to 2024 EPA AQS record was used to characterize $PM_{2.5}$ across Idaho. The regional climatology was found to be bimodal, with an August to September wildfire maximum and a November to February wood-smoke and inversion maximum separated by a clean spring background, and July to September carried 36.6 % of the annual mass, exceeding 50 % in severe fire years. It was found that the cold-season and background burdens declined significantly, at -0.9 and -0.7 µg m^{-3} per decade, while the fire season rose at 2.5 µg m^{-3} per decade, which left the annual mean flat. PCA separated the network into two sources, namely winter-peaking wood-combustion valley towns and summer-peaking wildfire-exposed background sites, while a temporal empirical orthogonal function identified a single state-wide and fire-season-dominated mode as the principal driver of regional variability. IDW surfaces localized the winter burden over the northern Silver Valley and the Salmon and Lemhi valley. With 32.7 % of site-years exceeding the 2024 annual standard, these results indicate that the two dominant $PM_{2.5}$ regimes of Idaho are diverging under a warming climate, and that season and source specific management is required to address both the winter and the fire-season burden.

DECLARATIONS

Acknowledgments

The author thanks the United States Environmental Protection Agency for public access to the Air Quality System database, and the Department of Physics, University of Idaho, for institutional support.

Authors' contributions

The author contributed solely to the article.

Availability of data and materials

The $PM_{2.5}$ data analyzed in this study are openly available from the United States Environmental Protection Agency Air Quality System (AQS) at https://www.epa.gov/aqs. The derived monthly, seasonal and site-level data products

generated during the study are available from the corresponding author upon reasonable request.

AI and AI-assisted tools statement

During the preparation of this work the author used a large language model (Claude; Anthropic, PBC) to assist with language editing, formatting and figure layout. These tools were not used to generate scientific insights or to analyze, interpret or draw conclusions from the data. The author reviewed and edited all content and takes full responsibility for the scientific content and for the published material.

Financial support and sponsorship

None.

Conflicts of interest

The author declared that there are no conflicts of interest.

Ethical approval and consent to participate

Not applicable.

Consent for publication

Not applicable.

Copyright

© The Author(s) 2026.

REFERENCES

[1] Kim, K.-H.; Kabir, E.; Kabir, S. A review on the human health impact of airborne particulate matter. *Environ. Int.* **2015**, *74*, 136-43.[DOI: 10.1016/j.envint.2014.10.005]

[2] Lelieveld, J.; Evans, J. S.; Fnais, M.; Giannadaki, D.; Pozzer, A. The contribution of outdoor air pollution sources to premature mortality on a global scale. *Nature* **2015**, *525*, 367-71.[DOI: 10.1038/nature15371]

[3] Di, Q.; Wang, Y.; Zanobetti, A.; et al. Air pollution and mortality in the Medicare population. *N. Engl. J. Med.* **2017**, *376*, 2513-22.[DOI: 10.1056/NEJMoa1702747]

[4] Brook, R. D.; Rajagopalan, S.; Pope, C. A.; et al. Particulate matter air pollution and cardiovascular disease: an update to the scientific statement from the American Heart Association. *Circulation* **2010**, *121*, 2331-78.[DOI: 10.1161/CIR.0b013e3181dbece1]

[5] Pope, C. A.; Dockery, D. W. Health effects of fine particulate air pollution: lines that connect. *J. Air Waste Manage. Assoc.* **2006**, *56*, 709-42.[DOI: 10.1080/10473289.2006.10464485]

[6] Anjum, M.; Siddique, N.; Younis, H.; et al. Chemometric assessment, seasonal variation and source apportionment of air pollutants in Islamabad's industrial area. *J. Trace Elem. Miner.* **2025**, *12*, 100244.[DOI: 10.1016/j.jtemin.2025.100244]

[7] Shah, M. H.; Shaheen, N.; Nazir, R. Assessment of the trace elements level in urban atmospheric particulate matter and source apportionment in Islamabad, Pakistan. *Atmos. Pollut. Res.* **2012**, *3*, 39-45.[DOI: 10.5094/APR.2012.004]

[8] Waheed, S.; Jaafar, M. Z.; Siddique, N.; Markwitz, A.; Brereton, R. G. PIXE analysis of PM2.5 and PM2.5-10 for air quality assessment of Islamabad, Pakistan: application of chemometrics for source identification. *J. Environ. Sci. Health, Part A* **2012**, *47*, 2016-27.[DOI: 10.1080/10934529.2012.695559]

[9] World Health Organization. *WHO global air quality guidelines: particulate matter (PM2.5 and PM10), ozone, nitrogen dioxide, sulfur dioxide and carbon monoxide;* World Health Organization: Geneva, 2021. https://www.who.int/publications/i/item/9789240034228

[10] U.S. Environmental Protection Agency. Reconsideration of the National Ambient Air Quality Standards for Particulate Matter (final rule). *Fed. Regist.* **2024**, *89*, 16202. https://www.federalregister.gov/d/2024-02637

[11] Abatzoglou, J. T.; Williams, A. P. Impact of anthropogenic climate change on wildfire across western US forests. *Proc. Natl. Acad. Sci. U. S. A.* **2016**, *113*, 11770-5.[DOI: 10.1073/pnas.1607171113]

[12] Jolly, W. M.; Cochrane, M. A.; Freeborn, P. H.; et al. Climate-induced variations in global wildfire danger from 1979 to 2013. *Nat. Commun.* **2015**, *6*, 7537.[DOI: 10.1038/ncomms8537]

[13] Balch, J. K.; Bradley, B. A.; Abatzoglou, J. T.; Nagy, R. C.; Fusco, E. J.; Mahood, A. L. Human-started wildfires expand the fire niche across the United States. *Proc. Natl. Acad. Sci. U. S. A.* **2017**, *114*, 2946-51.[DOI: 10.1073/pnas.1617394114]

[14] McClure, C. D.; Jaffe, D. A. US particulate matter air quality improves except in wildfire-prone areas. *Proc. Natl. Acad. Sci. U. S. A.* **2018**, *115*, 7901-6.[DOI: 10.1073/pnas.1804353115]

[15] Burke, M.; Driscoll, A.; Heft-Neal, S.; Xue, J.; Burney, J.; Wara, M. The changing risk and burden of wildfire in the United States. *Proc. Natl. Acad. Sci. U. S. A.* **2021**, *118*, e2011048118.[DOI: 10.1073/pnas.2011048118]

[16] Burke, M.; Childs, M. L.; de la Cuesta, B.; et al. The contribution of wildfire to PM2.5 trends in the USA. *Nature* **2023**, *622*, 761-6.[DOI: 10.1038/s41586-023-06522-6]

[17] O'Dell, K.; Ford, B.; Fischer, E. V.; Pierce, J. R. Contribution of wildland-fire smoke to US PM2.5 and its influence on recent trends. *Environ. Sci. Technol.* **2019**, *53*, 1797-804.[DOI: 10.1021/acs.est.8b05430]

[18] Aguilera, R.; Corringham, T.; Gershunov, A.; Benmarhnia, T. Wildfire smoke impacts respiratory health more than fine particles from other sources: observational evidence from Southern California. *Nat. Commun.* **2021**, *12*, 1493.[DOI: 10.1038/s41467-021-21708-0]

[19] Reid, C. E.; Brauer, M.; Johnston, F. H.; Jerrett, M.; Balmes, J. R.; Elliott, C. T. Critical review of health impacts of wildfire smoke exposure. *Environ. Health Perspect.* **2016**, *124*, 1334-43.[DOI: 10.1289/ehp.1409277]

[20] Chen, G.; Guo, Y.; Yue, X.; et al. Mortality risk attributable to wildfire-related PM2.5 pollution: a global time series study in 749 locations. *Lancet Planet. Health* **2021**, *5*, e579-e87.[DOI: 10.1016/S2542-5196(21)00200-X]

[21] Chen, H.; Samet, J. M.; Bromberg, P. A.; Tong, H. Cardiovascular health impacts of wildfire smoke exposure. *Part. Fibre Toxicol.* **2021**, *18*, 2.[DOI: 10.1186/s12989-020-00394-8]

[22] Holm, S. M.; Miller, M. D.; Balmes, J. R. Health effects of wildfire smoke in children and public health tools: a narrative review. *J. Expo. Sci. Environ. Epidemiol.* **2021**, *31*, 1-20.[DOI: 10.1038/s41370-020-00267-4]

[23] Naeher, L. P.; Brauer, M.; Lipsett, M.; et al. Woodsmoke health effects: a review. *Inhal. Toxicol.* **2007**, *19*, 67-106.[DOI: 10.1080/08958370600985875]

[24] Ward, T. J.; Lange, T. The impact of wood smoke on ambient PM2.5 in northern Rocky Mountain valley communities. *Environ. Pollut.* **2010**, *158*, 723-9.[DOI: 10.1016/j.envpol.2009.10.016]

[25] Silcox, G. D.; Kelly, K. E.; Crosman, E. T.; Whiteman, C. D.; Allen, B. L. Wintertime PM2.5 concentrations during persistent, multi-day cold-air pools in a

mountain valley. *Atmos. Environ.* **2012**, *46*, 17-24.[DOI: 10.1016/j.atmosenv.2011.10.041]

[26] Watson, J. G.; Chow, J. C. A wintertime PM2.5 episode at the Fresno, CA, supersite. *Atmos. Environ.* **2002**, *36*, 465-75.[DOI: 10.1016/S1352-2310(01)00309-0]

[27] Whiteman, C. D.; Hoch, S. W.; Horel, J. D.; Charland, A. Relationship between particulate air pollution and meteorological variables in Utah's Salt Lake Valley. *Atmos. Environ.* **2014**, *94*, 742-53.[DOI: 10.1016/j.atmosenv.2014.06.012]

[28] Ringner, M. What is principal component analysis? *Nat. Biotechnol.* **2008**, *26*, 303-4.[DOI: 10.1038/nbt0308-303]

[29] Thurston, G. D.; Spengler, J. D. A quantitative assessment of source contributions to inhalable particulate matter pollution in metropolitan Boston. *Atmos. Environ.* **1985**, *19*, 9-25.[DOI: 10.1016/0004-6981(85)90132-5]

[30] Paatero, P.; Tapper, U. Positive matrix factorization: a non-negative factor model with optimal utilization of error estimates of data values. *Environmetrics* **1994**, *5*, 111-26.[DOI: 10.1002/env.3170050203]

[31] Xie, Y.; Chen, T.-B.; Lei, M.; et al. Spatial distribution of soil heavy metal pollution estimated by different interpolation methods: accuracy and uncertainty analysis. *Chemosphere* **2011**, *82*, 468-76.[DOI: 10.1016/j.chemosphere.2010.09.053]

[32] Anjum, M.; Siddique, N.; Younis, H.; et al. Heavy metals and radionuclides in Islamabad's industrial area: a comprehensive analysis of soil and water pollution, source apportionment and health effects using statistical and geospatial tools. *J. Trace Elem. Miner.* **2024**, *8*, 100127.[DOI: 10.1016/j.jtemin.2024.100127]

[33] Mann, H. B. Nonparametric tests against trend. *Econometrica* **1945**, *13*, 245-59.[DOI: 10.2307/1907187]

[34] Sen, P. K. Estimates of the regression coefficient based on Kendall's tau. *J. Am. Stat. Assoc.* **1968**, *63*, 1379-89.[DOI: 10.1080/01621459.1968.10480934]

[35] Jaffe, D. A.; O'Neill, S. M.; Larkin, N. K.; et al. Wildfire and prescribed burning impacts on air quality in the United States. *J. Air Waste Manage. Assoc.* **2020**, *70*, 583-615.[DOI: 10.1080/10962247.2020.1749731]

[36] Childs, M. L.; Li, J.; Wen, J.; et al. Daily local-level estimates of ambient wildfire smoke PM2.5 for the contiguous US. *Environ. Sci. Technol.* **2022**, *56*, 13607-21.[DOI: 10.1021/acs.est.2c02934]

[37] Buchholz, R. R.; Park, M.; Worden, H. M.; Tang, W.; Edwards, D. P. New seasonal pattern of pollution emerges from changing North American wildfires. *Nat. Commun.* **2022**, *13*, 2043.[DOI: 10.1038/s41467-022-29623-8]

[38] Ahmad, S.; Zeb, B.; Ditta, A.; Alam, K.; Ahmad, I.; Usman, F. Seasonal variations of particulate matter in two size fractions (PM2.5 and PM10) and their relationship with meteorological parameters in Lahore, Pakistan. *Environ. Sci.: Adv.* **2025**, *4*, 1103-16.[DOI: 10.1039/D5VA00004A]

[39] Batterman, S.; Xu, L.; Chen, F.; Chen, F.; Zhong, X. Characteristics of PM2.5 concentrations across Beijing during 2013-2015. *Atmos. Environ.* **2016**, *145*, 104-14.[DOI: 10.1016/j.atmosenv.2016.08.060]

[40] Guttikunda, S. K.; Dammalapati, S. K.; Pradhan, G.; Krishna, B.; Jethva, H. T.; Jawahar, P. What is polluting Delhi's air? A review from 1990 to 2022. *Sustainability* **2023**, *15*, 4209.[DOI: 10.3390/su15054209]

[41] Miranda, R. M.; Andrade, M. D. F.; Fornaro, A.; Astolfo, R.; Andre, P. A.; Saldiva, P. Urban air pollution: a representative survey of PM2.5 mass concentrations in six Brazilian cities. *Air Qual. Atmos. Health* **2012**, *5*, 63-77.[DOI: 10.1007/s11869-010-0124-1]

[42] Atuyambe, L. M.; Etajak, S.; Walyawula, F.; Ssematimba, J.; Okure, D.; Bainomugisha, E. Air quality and attributable mortality among city dwellers in Kampala, Uganda: results from 4 years of continuous PM2.5 concentration monitoring using BAM 1022 reference instrument. *J. Expo. Sci. Environ. Epidemiol.* **2025**, *35*, 288-93.[DOI: 10.1038/s41370-024-00684-9]

[43] Lonati, G.; Giugliano, M.; Ozgen, S. Primary and secondary components of PM2.5 in Milan (Italy). *Environ. Int.* **2008**, *34*, 665-70.[DOI: 10.1016/j.envint.2007.12.009]

[44] Badami, M. M.; Aldekheel, M.; Aghaei, Y.; Sioutas, C. Trends in fine particulate matter and source contributions over the last decade in central Los Angeles (2014-2024): policy-driven declines, COVID-19 disruptions, and wildfires. *Atmos. Environ.* **2025**, *360*, 121421.[DOI: 10.1016/j.atmosenv.2025.121421]

[45] O'Dell, K.; Bilsback, K.; Ford, B.; et al. Estimated mortality and morbidity attributable to smoke plumes in the United States: not just a western US problem. *GeoHealth* **2021**, *5*, e2021GH000457.[DOI: 10.1029/2021GH000457]